Supporting Information

Mineralized aggregates based on native protein phase transition for non-destructive diagnosis of seborrheic skin by surface-enhanced Raman spectroscopy

Hao Liu,[1] Zhiming Liu,[2] Hao Zhang,[1] Ke Huang,[1] Xiaohui Liu,[1] Hui Jiang,[1,*] and Xuemei Wang,[1,*]

[1] State Key Laboratory of Digital Medical Engineering, School of Biological Science and Medical Engineering, Southeast University, Nanjing, Jiangsu 210096, China

[2] Guangdong Provincial Key Laboratory of Laser Life Science & Guangzhou Key Laboratory of Spectral Analysis and Functional Probes, College of Biophotonics, South China Normal University, Guangzhou 510631, P.R. China

[*] Corresponding author:

xuewang@seu.edu.cn (Dr. Xuemei Wang); sungi@seu.edu.cn (Dr. Hui Jiang);

Supporting Figure

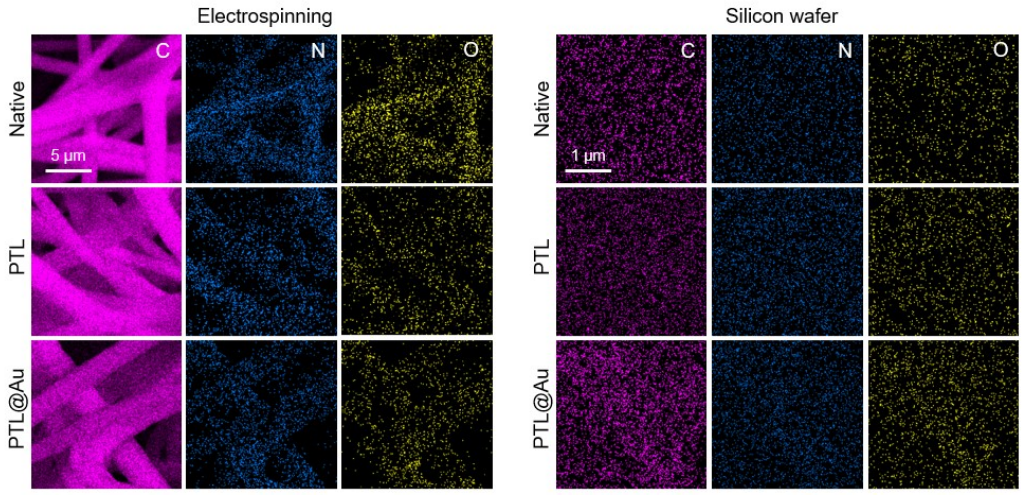

Figure S1. Scanning electron microscopy (SEM) images of electrospinning and silicon wafers after different treatments (PTL and PTL@Au) and the corresponding elemental mappings. (C, N, and O).

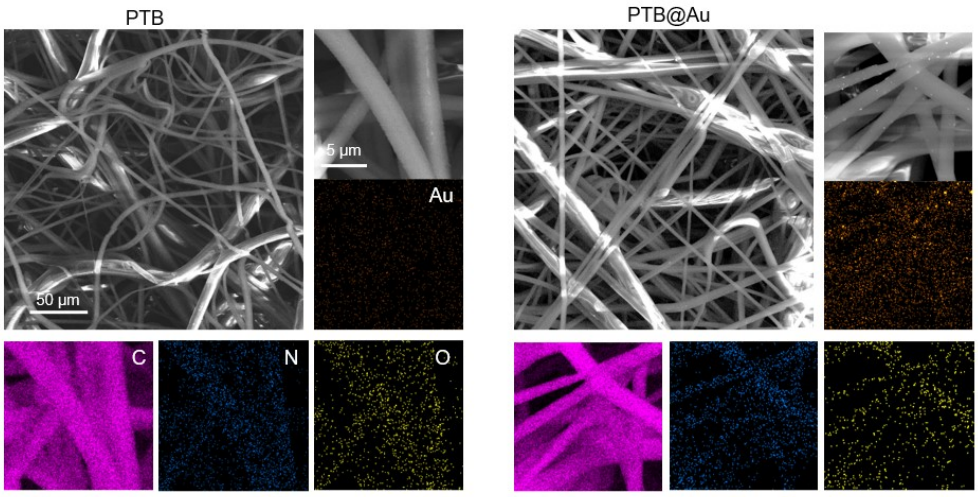

Figure S2. SEM of electrospinning after different treatments (PTB and PTB@Au) and the corresponding elemental mappings. (Au, C, N, and O).

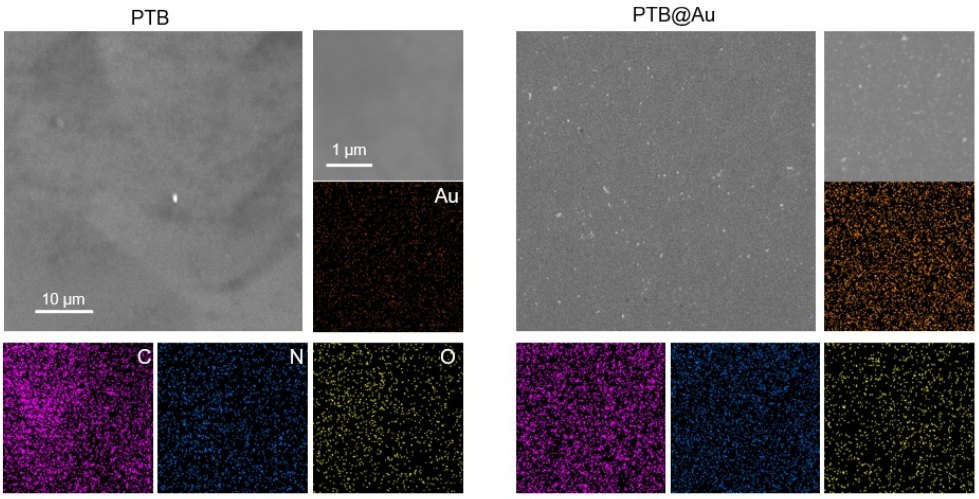

Figure S3. SEM of silicon wafers after different treatments (PTB and PTB@Au) and their elemental mappings. (Au, C, N, and O).

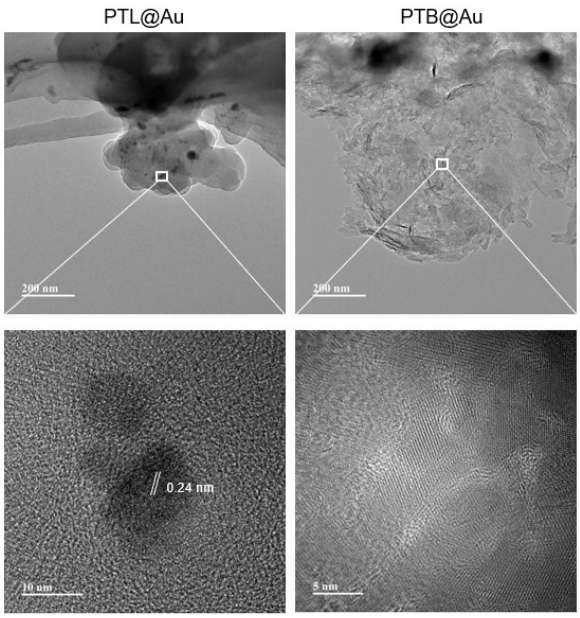

Figure S4. TEM and high resolution-TEM (HRTEM) of PTL@Au and PTB@Au.

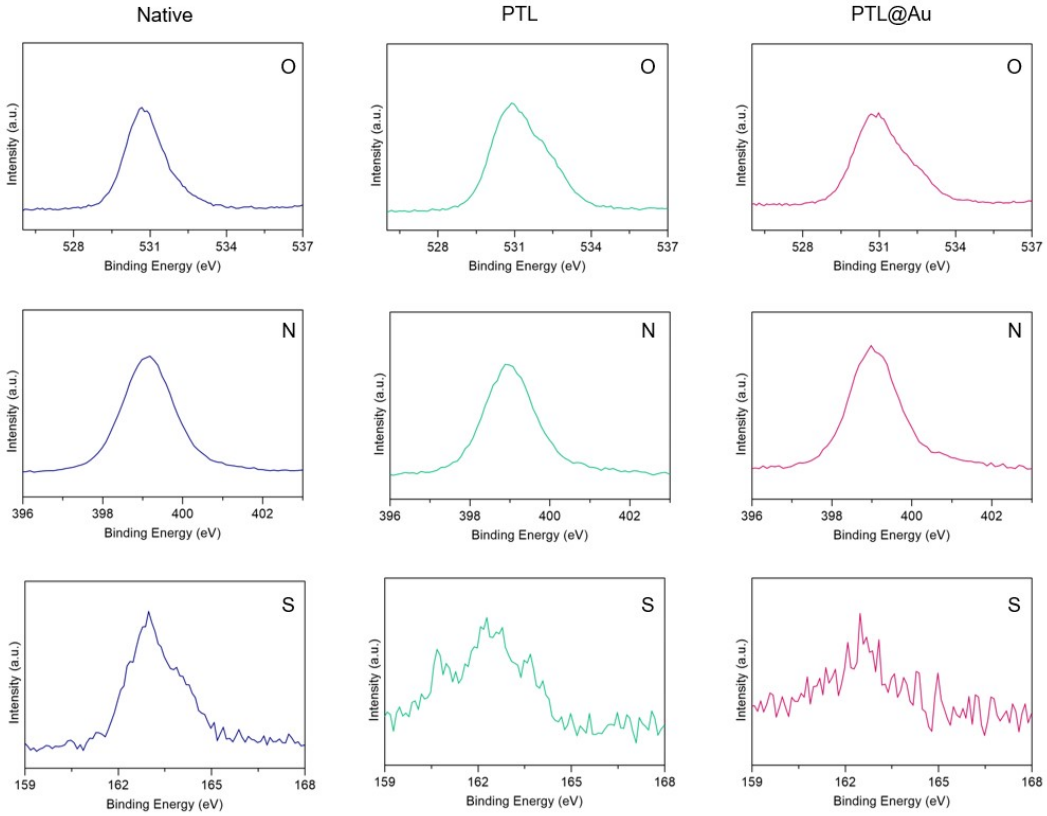

Figure S5. The high-resolution X-ray photoelectron spectroscopy (XPS) of O 1s, N 1s, and S 2p spectra.

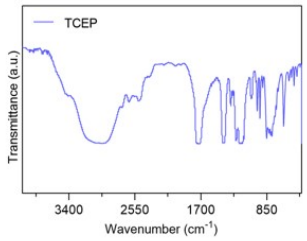

Figure S6. The Fourier transform infrared spectra (FT-IR) of Tris(2-carboxyethyl)phosphine (TCEP).

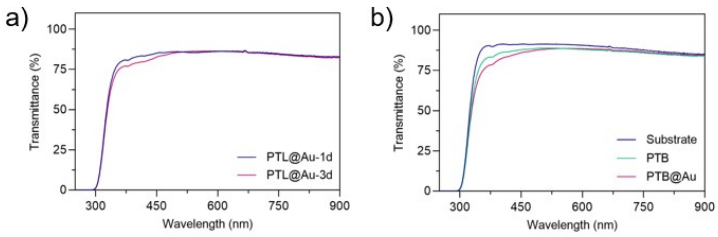

Figure S7. a) The optical transmittance of PTL@Au on quartz glass after different incubation times with Au (III). b) The optical transmittance of PTB and PTB@Au on quartz glass.

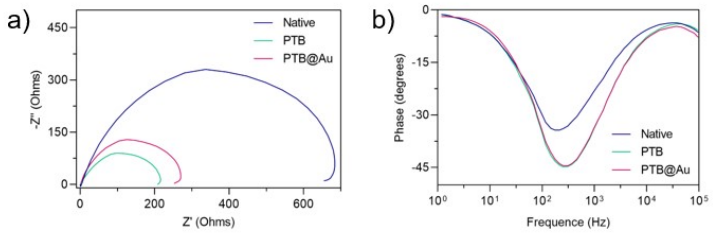

Figure S8. a) Nyquist plot of electrospinning, PTB, and PTB@Au. b) The corresponding phase angle of electrodes impedance as a function of the frequency.

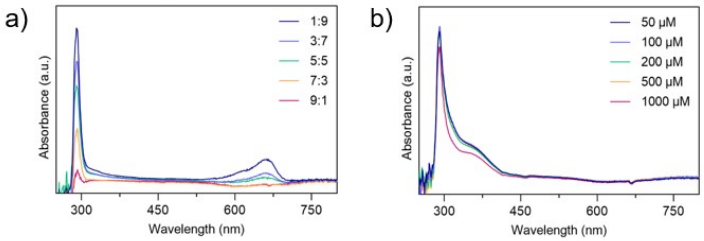

Figure S9. a) The UV-vis absorption spectra of TCEP and lysozyme mixed with different volume ratios. b) The UV-vis absorption spectra of the same volume ratio (TCEP / lysozyme = 1 / 1) solution of incubation with different concentration of Au (III) after 72 hours.

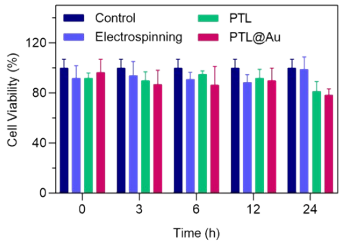

Figure S10. Cell viability of LO2 cell after incubation with PTL and PTL@Au.

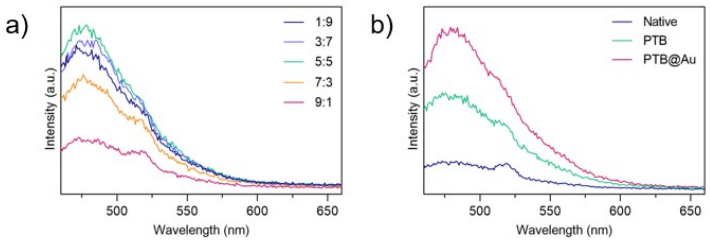

Figure S11. a) Fluorescence emission (Em) spectra of thioflavin T (The final concentration is 30 μM) after incubation of TCEP and lysozyme mixed with different volume ratios. b) Em spectra of thioflavin T after incubation of BSA, PTB, and PTB@Au.

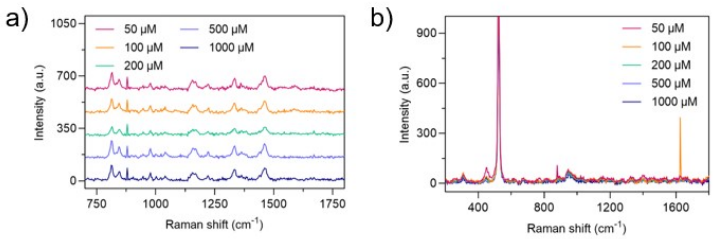

Figure S12. Raman spectra of a) electrospinning and b) silicon wafers with PTL@Au at different concentration of Au (III).

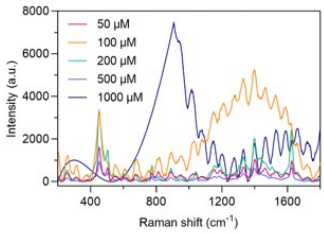

Figure S13. Surface-enhanced Raman spectra (SERS) of methylene blue (MB) on PTB@Au at different concentration of Au(III).

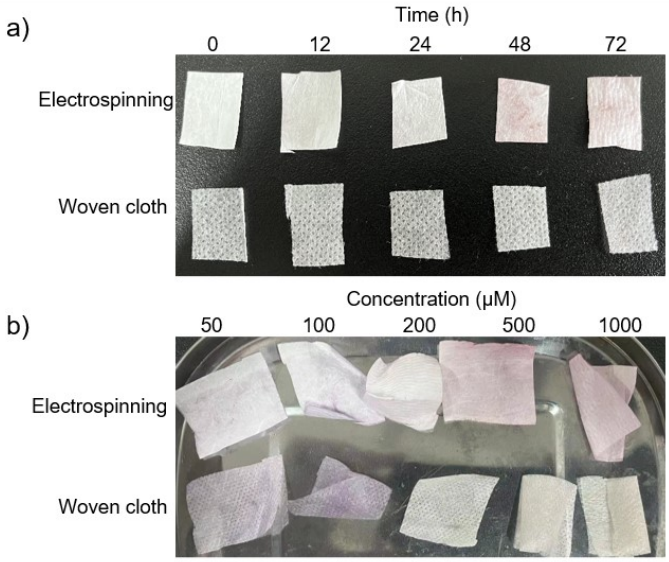

Figure S14. Digital photos of substrate materials (Electrospinning and woven cloth) modified with PTL@Au at a) different incubation time and b) different concentration of Au(III). The concentration of gold ions is 200 μM.

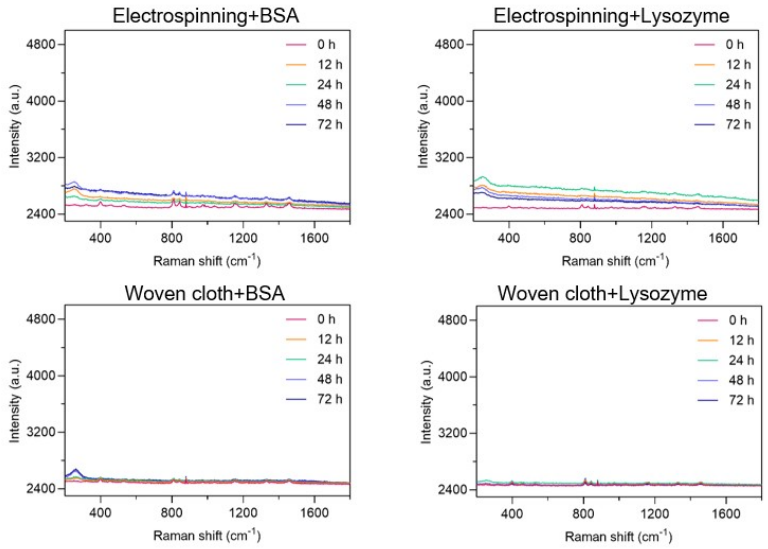

Figure S15. Raman spectra of electrospinning and woven cloth with PTL@Au and PTB@Au at different incubation time of Au (III). The concentration of gold ions is 200 μM.

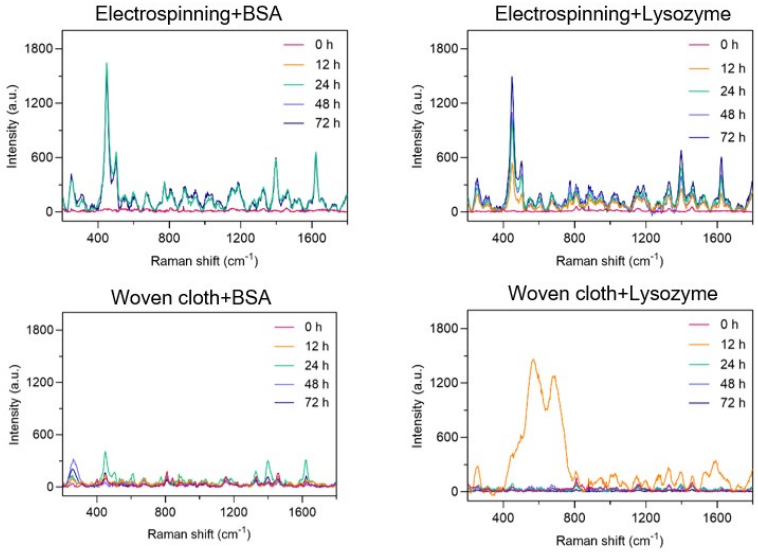

Figure S16. Surface-enhanced Raman spectra (SERS) of methylene blue (MB) on electrospinning and woven cloth with PTL@Au and PTB@Au at different incubation time of Au (III). The concentration of gold ions is 200 μM.

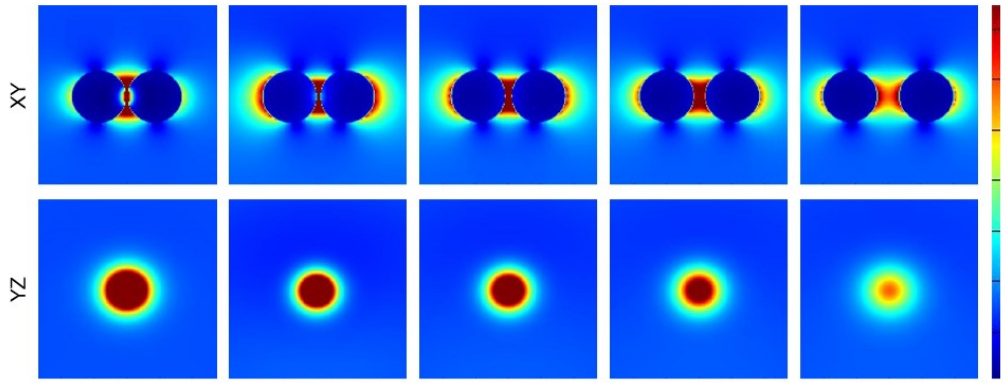

Figure S17. Electric field simulation of gold nanoparticles in XZ and YZ directions under 785 nm excitation. Gold nanoparticles are arranged horizontally on the X-axis.

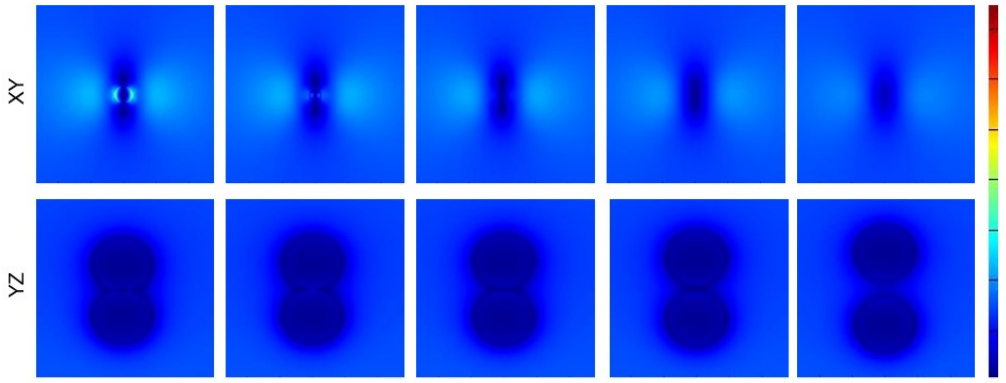

Figure S18. Electric field simulation of gold nanoparticles in XZ and YZ directions under 785 nm excitation. Gold nanoparticles are arranged horizontally in the Z-axis.

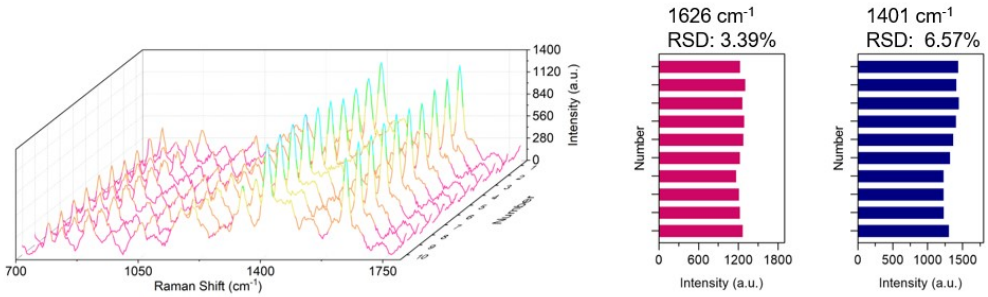

Figure S19. Repeatability of SERS of MB (10^{-5} M) on electrospinning with PTB@Au and the intensity and RSD of the Raman band at 1401 and 1626 cm^{-1}.

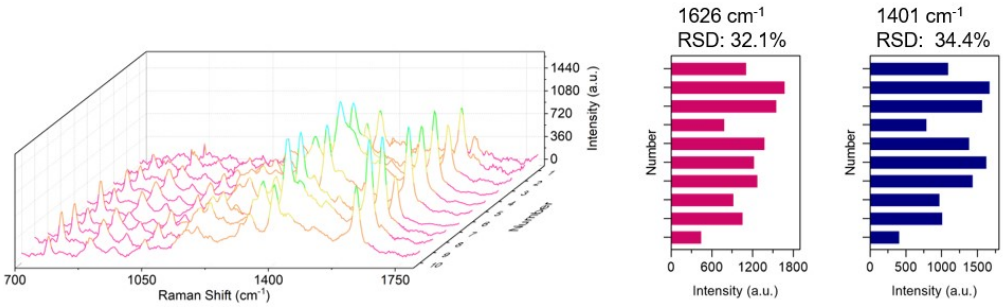

Figure S20. Repeatability of SERS of MB (10^{-5} M) on stainless steel with PTB@Au and the intensity and RSD of the Raman band at 1401 and 1626 cm^{-1}.

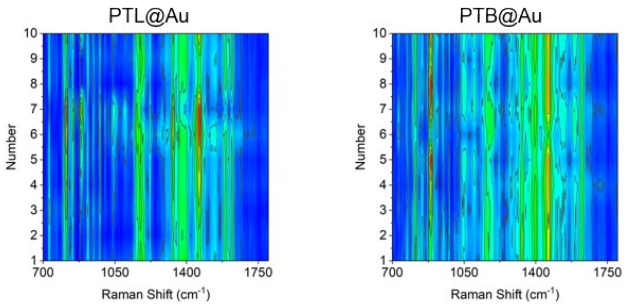

Figure S21. Repeatability of SERS of crystal violet (CV, 10^{-5} M) on electrospinning with PTL@Au and PTB@Au.

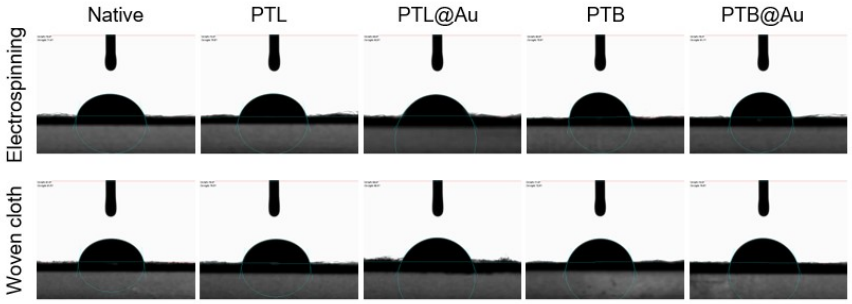

Figure S22. Representative microscopic digital photos of static droplets of squalene on the substrate.

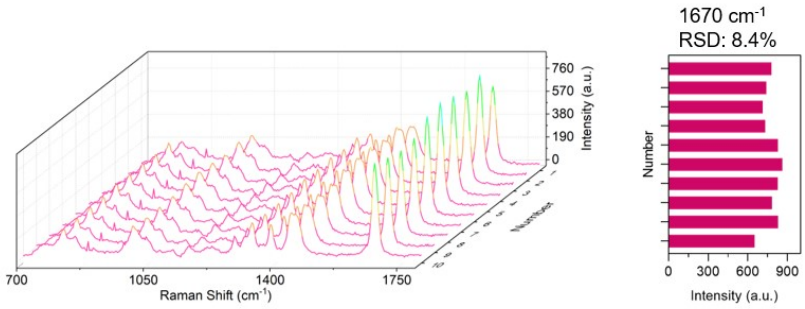

Figure S23. Repeatability of SERS of squalene (10^{-5} M) on electrospinning with PTB@Au and the intensity and RSD of the Raman band at 1670 cm^{-1}.